Available online at www.sciencedirect.com

SCIENCE DIRECT®

Vision Research 46 (2006) 117–128

Vision Research

www.elsevier.com/locate/visres

Quantification of stato-kinetic dissociation by semi-automated perimetry

Jan Schiller [a], Jens Paetzold [a], Reinhard Vonthein [b], William M. Hart [c], Anne Kurtenbach [a], Ulrich Schiefer [a,*]

[a] *University Eye Hospital Tuebingen, Department II, Schleichstrasse 12-16, D-72076 Tuebingen, Germany*
[b] *University of Tuebingen, Department of Medical Biometry, Westbahnhofstrasse 55, D-72070 Tuebingen, Germany*
[c] *Washington University, School of Medicine, 660 South Euclid Avenue, St. Louis, MO 63110, USA*

Received 13 October 2004; received in revised form 22 August 2005

Abstract

The difference in threshold sensitivities that are found when examining the visual field (VF) with static versus kinetic perimetric methods is called stato-kinetic dissociation (SKD). In this pilot study, we describe a semi-automated procedure for quantifying SKD. Fifteen patients with VF defects were examined with kinetic and static perimetry. SKD values were defined as positive when the static scotoma was larger than the kinetic one. We found significant local variations of SKD along scotoma borders with the individual reaction time as an important criterion when determining kinetic thresholds. There was a verifiable SKD in all patients with locally negative values in eight subjects.

Keywords: Semi-automated perimetry; Stato-kinetic dissociation; Reaction time

1. Introduction

In 1917 George Riddoch, a British military physician, first described a visual phenomenon which he found in soldiers that had sustained injuries to the occipital lobe during the first world war. These men had restricted visual fields and they reported an unexpected feature to their visual loss. Objects presented in the "blind" hemifield were invisible when kept stationary, but were immediately detectable when moved (Riddoch, 1917). Riddoch examined 10 patients and concluded from his observations that there is a segregation of visual processing for moving and stationary objects at the level of the primary visual cortex. He concluded that this stato-kinetic dissociation (SKD) was limited to lesions of the occipital cortex and that an absence of SKD was a poor prognostic sign.

However, in 1971 Zappia et al. described two patients in whom SKD was found in the absence of cortical disease: one patient suffered from a large aneurysm of the left internal carotid artery, compressing the left optic tract, and the other patient had a large tumor that displaced the optic chiasm and compressed the right optic nerve (Zappia, Enoch, Stamper, Winkelman, & Gay, 1971). These observations showed that the phenomenon first described by Riddoch is not specific for retrogeniculate disease.

Several subsequent studies have since shown that SKD appears in nearly all classes of diseases that damage the afferent visual pathways, and can even be detected in healthy subjects (Charlier, Defoort, Rouland, & Hache, 1989; Finkelstein & Johnson, 1989; Gandolfo, 1996; Gandolfo, Rossi, Ermini, & Zingirian, 1995; Hudson & Wild, 1992; Katsumori, Bun, Shirabe, & Mizokami, 1991; Krastel, Auffarth, Glaser, Beitzinger, & Alexandridis, 1996; Osako, Casson, Johnson, Huang, & Keltner, 1991; Riddoch, 1917; Safran & Glaser, 1980; Tsutsui, Ichihashi, & Kimura, 1984; Wedemeyer, Johnson, & Keltner, 1989; Yabuki, Sakai, Suzumura, Endo, & Matsuo, 1989; Zappia et al., 1971). The dissociation might be a consequence of separate, or partially separate, processing of kinetic and

* Corresponding author. Tel.: +49 7071 29 87429; fax: +49 7071 29 5038.
E-mail address: ulrich.schiefer@med.uni-tuebingen.de (U. Schiefer).

0042-6989/$ - see front matter © 2005 Elsevier Ltd. All rights reserved.
doi:10.1016/j.visres.2005.08.026

static information, which begins in the retina (Safran & Glaser, 1980): the magnocellular (M) system is generally more sensitive to high temporal frequencies and low spatial frequencies, and the parvocellular (P) system is more sensitive to stimuli with low temporal and high spatial frequencies (Lee, 1993). SKD may therefore indicate a selective damage to one or other of these systems and may be a helpful tool for the diagnosis and prognosis of visual field loss.

It has been proposed that the M system has a more global function in the interpretation of spatial perception, whereas the P system is more involved in the analysis of (color) information of stationary objects (Livingstone & Hubel, 1984, 1988; Merigan & Maunsell, 1990). A functional specialization of visual information would explain the finding that impairment of the visual pathway or higher visual areas does not always affect all qualities of visual perception: If some attributes of the visual image are processed predominantly by one pathway and if there is a parallel processing in subdivided pathways (Benevento & Yoshida, 1981; Bullier & Kennedy, 1983; Cowey & Stoerig, 1991; ffytche, Guy, & Zeki, 1995; Yukie & Iwai, 1981; Zeki, 1978), a selective destruction of one pathway would lead to typical perceptual deficiencies, However, further experimental data imply that the function of M and P pathways is not as separate as initially proposed and that there is some extent of overlap between the two systems (Lee, 1993).

The M and P systems both belong to the thalamofugal pathway, the main pathway for visual information to reach the cortex. However, there are other visual pathways—the accessory optical system and the tectofugal pathway—which may also play a role in SKD: The loss of visual information because of a damaged parvocellular system might be compensated, at least in part, by one of these accessory pathways (Barbur, Watson, Frackowiak, & Zeki, 1993; Cowey & Stoerig, 1991; ffytche et al., 1995; ffytche, Guy, & Zeki, 1996; Weiskrantz, Warrington, Sanders, & Marshall, 1974; Weiskrantz, 1996; Zeki & ffytche, 1998; Zihl, 1980).

Among the studies cited above only a few have attempted to quantify the extent of SKD. In none of these studies was the spatial distribution of SKD along a scotoma border examined both qualitatively as well as quantitatively, and with the use of a single instrument. The purpose of this study was to develop a semi-automated method for detecting and quantifying the spatial distribution of SKD at the margins of various types of visual field defects. Future studies will be aimed at examining its prognostic power and relevance as a diagnostic tool.

2. Methods and subjects

2.1. Patients

Three groups of patients with advanced, stable visual field defects were examined. There were five patients in each group for a total of fifteen. Each group consisted of five patients with one of the following disorders: (1) glaucoma, (2) retinitis pigmentosa, and (3) retrogeniculate disease (Table 1). These disorders were chosen to select representative pathologies, affecting the neuronal chain of the visual pathway(s) at three different levels (retina, optic nerve, post-geniculate segment).

2.2. Perimetric parameters

To estimate the test reliability, one patient in each group was examined at two separate times. One patient with retinitis pigmentosa was tested three times. Thus, 11 patients were examined once, 3 patients were examined twice, and 1 patient was examined three times. In sum, there were 20 examinations, each with kinetic and static perimetric methods. All examinations were carried out with the Tuebingen

Table 1
Visual field characteristics of the patients examined in this study

Patient	Age	Lesion	Visual field defect
C.H.	57	Glaucoma	Stage IV (Aulhorn classification[a])
E.N.	54	Glaucoma	Stage III
G.W.	76	Glaucoma	Stage III
H.F.	71	Glaucoma	Stage III
J.B.	54	Glaucoma	Stage IV
J.W.	36	Retinitis pigmentosa	Concentric visual field defect with a residual visual field of ~20°
L.A.	69	Retinitis pigmentosa	Concentric visual field defect with a residual visual field of ~10°
L.B.	37	Retinitis pigmentosa	Concentric visual field defect with a residual visual field of ~15°
S.K.	43	Retinitis pigmentosa	Concentric visual field defect with a residual visual field of ~10°
T.M.	45	Retinitis pigmentosa	Concentric visual field defect with a residual visual field of ~20°
B.B.	34	Intracranial hemorrhage arising from a left partial arteriovenous malformation	Complete quadrantanopia of the right lower quadrant
E.F.	59	Intracranial hemorrhage arising from hypertension	Complete quadrantanopia of the left upper quadrant
I.M.	40	Apoplexia of the left posterior cerebral artery	Incomplete quadrantanopia of the right upper quadrant
M.S.	50	Apoplexia of both posterior cerebral arteries	Complete quadrantanopia of the right upper quadrant
T.M.	22	Intracranial hemorrhage arising from a cavernous angioma	Complete quadrantanopia of the right lower quadrant and incomplete quadrantanopia of the right upper quadrant

[a] Aulhorn and Karmeyer (1977).

Computer Campimeter (TCC) (Schiefer & Stercken-Sorrenti, 1993; Wabbels, Schiefer, Treutwein, Benda, & Strecken-Sorrenti, 1995) using a calibrated, high resolution, true-color video display unit (Calibrator, BARCO, Kortriyk, Belgium) (Dietrich, Selig, Friedrich, Benda, & Schiefer, 1996). With this instrument, visual fields can be examined out to 34° of eccentricity in the horizontal meridian and up to 25° eccentricity in the vertical meridian. By shifting the fixation point, additional peripheral visual field areas can also be examined. The stimulus characteristics for all examinations—manual as well as automated perimetry—were identical: 26′ in size, and 110 cd/m^2 in luminance, (equivalent to the Goldmann stimulus III3e) with a background luminance of 10 cd/m^2.

2.3. Perimetric procedures

In an initial session, the border of the scotoma was roughly estimated by manual kinetic and static perimetry (Figs. 1A and 2A). In the manual kinetic mode, the angular velocity of stimulus movement was about 2–3°/s and in the static mode stimulus presentation duration was about 200 ms.

Based on the results of the initial session, two sets of perimetric vectors were constructed—one for an automated static and the other for an automated kinetic examination. Kinetic vectors were defined as straight line segments, each having an origin and a termination, and along which the stimulus was moved. In each examination, a set of kinetic vectors consisted of 16–24 vectors (length 6° each), which started approximately 2–3° within the scotoma and crossed the scotoma border as perpendicularly as possible. In the kinetic mode at least four additional vectors were presented within intact portions of the visual field to estimate the individual reaction time for each patient (Fig. 1B). Each static examination vector (length 6°) consisted of five stimulus locations in a linear arrangement. The distance between two stimulus locations on such a vector was 1.5° (Fig. 2B). The static set of vectors consisted of the same number of vectors as the kinetic set and had in almost all cases the same orientation. If higher SKD was encountered in the initial session, the locations assigned to the static/kinetic vectors were more widely separated. In the subsequent automated examination each stimulus was presented six times in a random order for each vector in the kinetic as well as in the static mode. All examinations were carried out with only one stimulus characteristic as mentioned before (26′ in size and 110 cd/m^2).

Patients' responses in automated kinetic perimetry were corrected for mean individual reaction time, estimated along the suprathreshold reaction time vectors. A "local kinetic threshold" (MEAN) and a related parameter for dispersion (SD) were determined (Fig. 1C).

In the automated static mode, because of the use of only one stimulus characteristic, local thresholds were estimated as positions on a vector assuming a probit model. Dispersion was assessed by computing the steepness of the "fre-

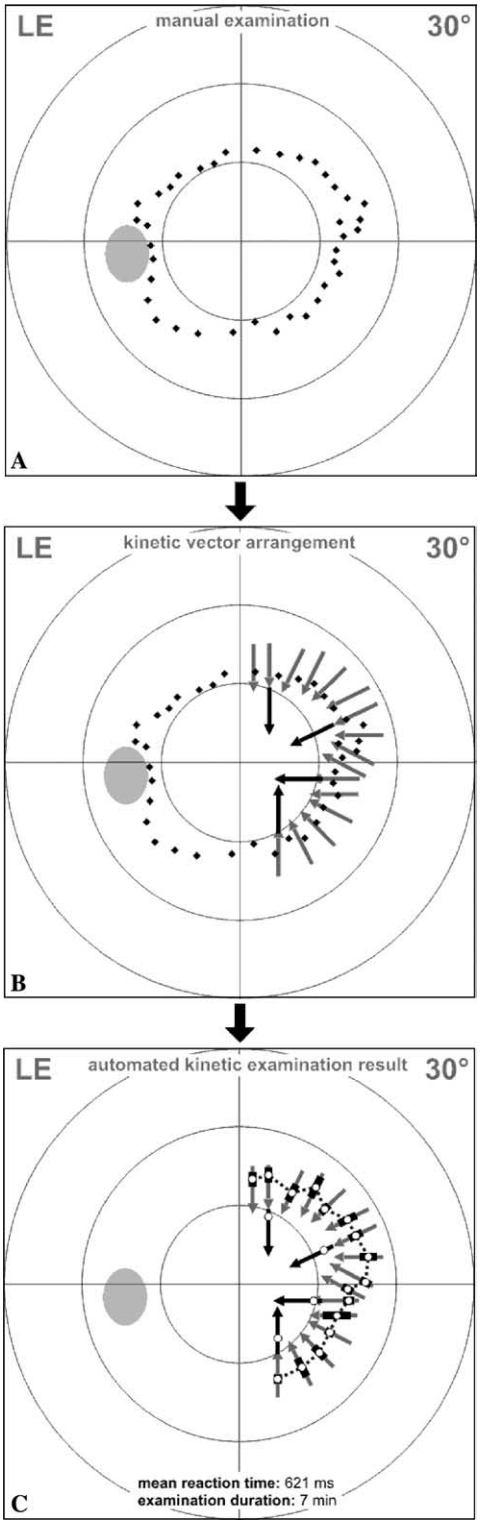

Fig. 1. (A) In an initial session, the location of the scotoma border is estimated by conventional manual kinetic and static perimetry. Each rhomb labels a kinetic or static threshold. (B) Kinetic vector arrangement. The gray arrows are vectors to evaluate the scotoma border, the black ones are vectors to measure individual reaction time. (C) Result of the automated kinetic examination. Each stimulus is presented six times in a random order. Each white dot represents a local kinetic threshold (MEAN), each black box represents the related parameter for dispersion (SD). Patients' responses are corrected for mean individual reaction time.

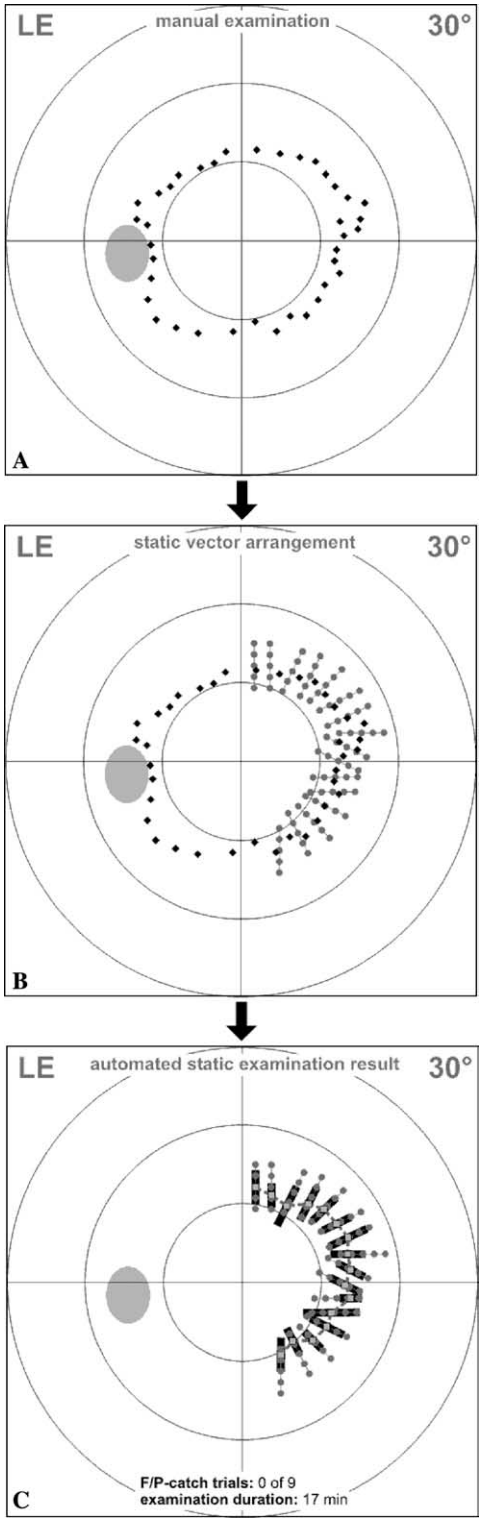

Fig. 2. (A) As in the kinetic examination part the conventional manual kinetic and static perimetry is used as basis for designing the static vector arrangement. Each rhomb labels a kinetic or static threshold. (B) Static vector arrangement. Each static "vector" consists of five static stimulus locations with an interstimulus distance of 1.5°. (C) Result of the automated static examination. Each stimulus is presented six times in a random order. Additionally, 4% false-positive catch trials are presented. Local thresholds are estimated as position on a vector assuming a probit model. Dispersion is assessed by evaluating the steepness of the "frequency-of-seeing curve" at the position of the located static threshold.

quency-of-seeing curve" at the location of each static threshold (Fig. 2C). As a result the static threshold is not measured by varying stimulus *intensity* at a certain visual field localisation but by varying the stimulus *localisation* with fixed stimulus intensity.

2.4. Perimetric data processing

A local measure of SKD was computed as the distance between the static scotoma borders and the corresponding kinetic ones (Fig. 3A). SKD was thus positive, if the static scotoma was larger than the kinetic one, otherwise it was given a negative value.

When comparing the distances between two borders that do not have identical shapes and/or orientations, connecting line segments with (artifactually) high values will be found at locations where a local indentation in one scotoma border is not matched by a similar shape in the other. A similar problem is encountered when measuring the width of a river, when standing on one bank and measuring the distance to the opposite side (see Fig. 3B). The measurement will be affected by the choice of a corresponding location on the other bank. How should this location be chosen?

Individual SKD values can be quantified along a scotoma border by subdividing each linear connection between two kinetic or two static thresholds into 20 equidistant points (Fig. 3C). The individual SKD is assessed by estimating the shortest distance between one of these points (e.g., on the connection of two static thresholds) and a corresponding (in this example kinetic) threshold on the other "bank" (Fig. 3D). This procedure is done for each point on each scotoma line. In this way, an artifactually high SKD—caused by incongruous courses of the scotoma borders as determined by the kinetic and static examinations—was avoided: SKD might be (marginally) underestimated but not overestimated.

This procedure was carried out for each estimate along the kinetic and static threshold contours. Plotting these values as corresponding ordinal pairs produced two graphs: one showing the SKD based on the kinetic thresholds and the other based on the static threshold values (Fig. 3E). The graphs illustrate the quantification of the resulting SKD values. The differing values depicted by these two graphs illustrate the comparability of estimates produced by this algorithm.

To minimize biasing of values caused by variable reaction times, an algorithm for excluding excessively high reaction times was developed. A loss of concentration might be the cause for such an outlier. This judgement has to be individual, since there can be a wide *inter*individual variation in reaction times. A *general* upper limit for reaction times cannot be used, since each individual has his or her own unique reaction time and the difference between two individuals can be systematically large. An algorithm was used to exclude responses that came after an imposed time limit. This algorithm (upper 75% quartile + 1.5∗ interquartile range of ln RT) was used to eliminate all responses with reaction times above the individually assigned upper limit.

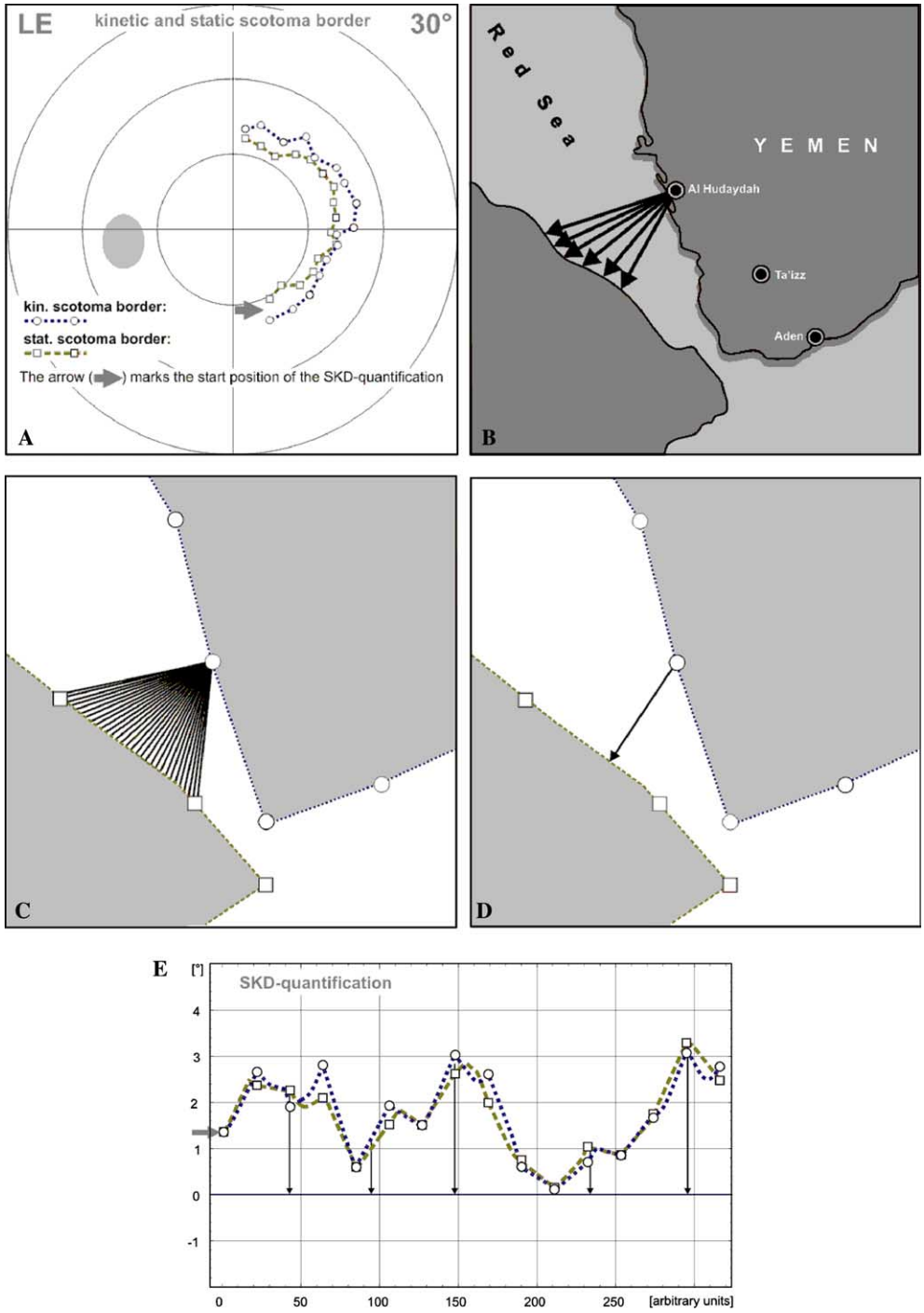

Fig. 3. (A) Scotoma borders evaluated by the automated kinetic (white dots and black broken line) and automated static examination (gray boxes and gray broken line). The arrow marks the reference position from where automated evaluation of stato-kinetic dissociation is started. (B) Estimating the stato-kinetic dissociation is like estimating the width of waters, rivers or lakes: One bank is the connection of the static thresholds, the other bank represents the connection of the kinetic thresholds. Starting from one point one has to choose a corresponding point on the opposite side of the river or lake. *Problem*: How to choose this point! Is it the shortest connection to the other side? Is the proper connection a perpendicular line starting from the position you are actually located? And what if the bank of the lake is full of windings like the southern part of the Red Sea? *Solution*: Each linear connection between two kinetic or two static thresholds is subdivided into 20 equidistant points. (C) The individual stato-kinetic dissociation is assessed by estimating the shortest distance between one of these points and one point on the other "bank". (D) This procedure is done with each point on each scotoma line. The calculation of the SKD is done basing on the "static bank" and on the "kinetic bank", respectively. In cases of an artificially large SKD (e.g., caused by crossings and turns of the scotoma "banks") based on one scotoma line, the result can be corrected by using the result basing on the other scotoma border. (E) Automated evaluation and visualization of SKD. Each *y*-value represents the local SKD, each dot (kinetic) or box (static) represents the position of an estimated threshold. The broken lines are not just connections between these thresholds. The black line shows calculated SKD based on the kinetic scotoma border, while the gray one is based on the static scotoma border. The arrow marks the reference position from where automated evaluation of stato-kinetic dissociation is started (see A).

In each static examination 2–5% false-positive catch trials (using an exclusively acoustic stimulus not followed by a visual stimulus) were presented. Before the beginning of the static examination it was pointed out to each patient that it is part of this examination technique that half of all stimuli are presented within the scotoma and therefore cannot be seen by the patient. Patients were instructed to press the button only when they were certain that they had seen the stimulus light.

3. Results

3.1. Patients

Typical results for each group of patients—retinitis pigmentosa, glaucoma, and lesions of the posterior pathway—are illustrated as follows:

Figs. 4A–E show the values determined for a patient (female; 57 years) with arcuate glaucomatous visual field

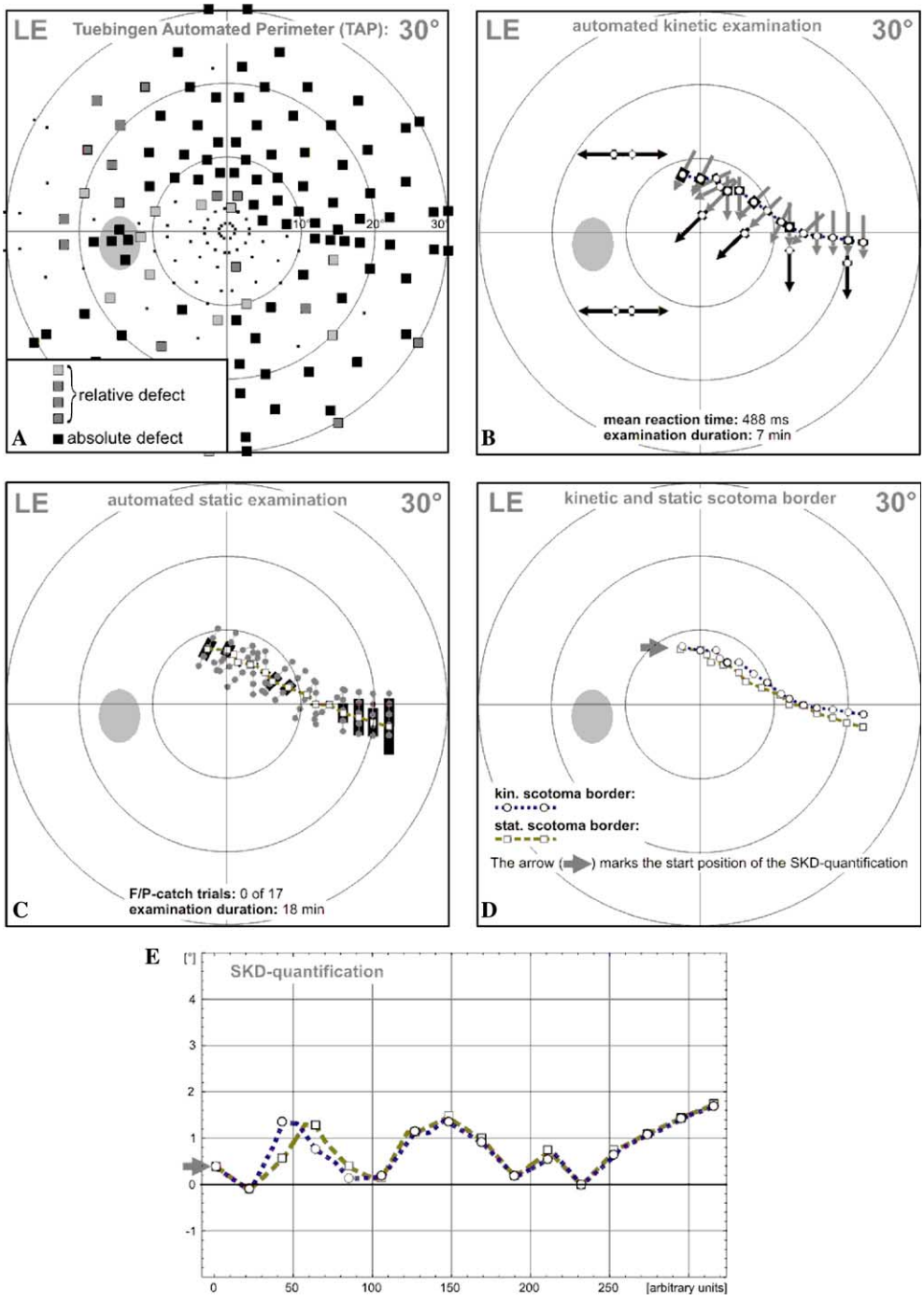

Fig. 4. Arcuate visual field defect of a patient suffering from glaucoma. (A) Standard visual field: threshold oriented, slightly supraliminal perimetry (Tuebingen automated perimeter, TAP); (B) automated kinetic examination; (C) automated static examination; (D) comparison of kinetic and static examination result; (E) graph of SKD quantification.

defects in the upper and lower hemifield, who demonstrated severe visual field loss when examined with routine automated static grid perimetry (Tuebingen Automated Perimeter: threshold oriented, slightly supraliminal automated perimetry, 30° visual field). She suffered from a longstanding loss of vision caused by normal tension glaucoma in both eyes. To minimize the examination time, the scotoma border was plotted for only a portion of its extent. Examinations with the TCC found only moderate values for SKD with a minimum of −0.1° (local negative SKD) and a maximum of 1.8°.

Figs. 5A–E illustrate the results for a patient (female; 43 years) suffering from retinitis pigmentosa, first diagnosed in 1988. Over the past several years there has been no progression of her visual field loss. Because of the small size of the remaining visual field, a reduction in the number of reaction time vectors was necessary. The

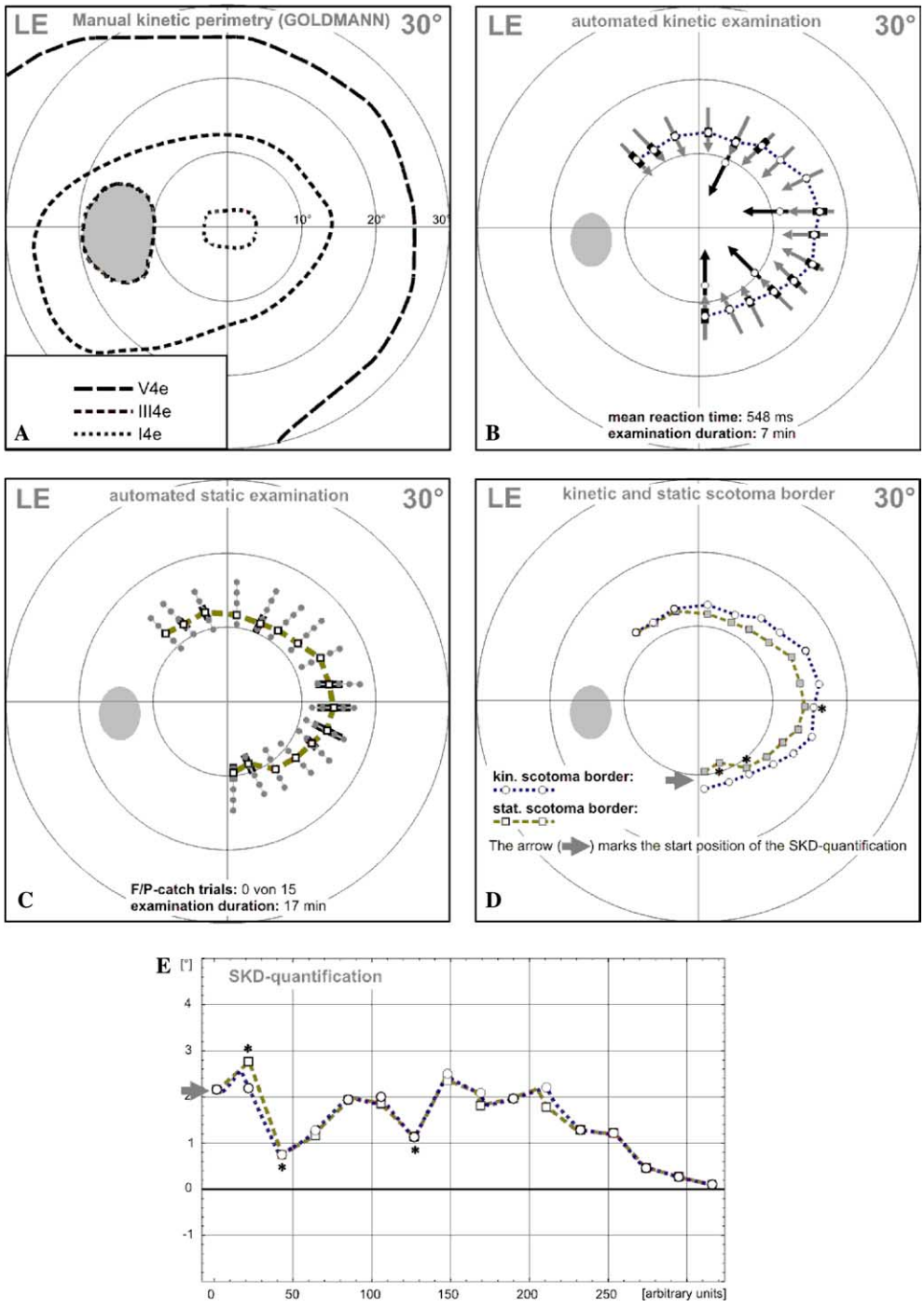

Fig. 5. Typical visual field defect of a patient with retinitis pigmentosa. (A) Standard visual field: manual kinetic perimetry (GOLDMANN-Perimeter); (B) automated kinetic examination; (C) automated static examination; (D) comparison of kinetic and static examination result; (E) graph of SKD quantification.

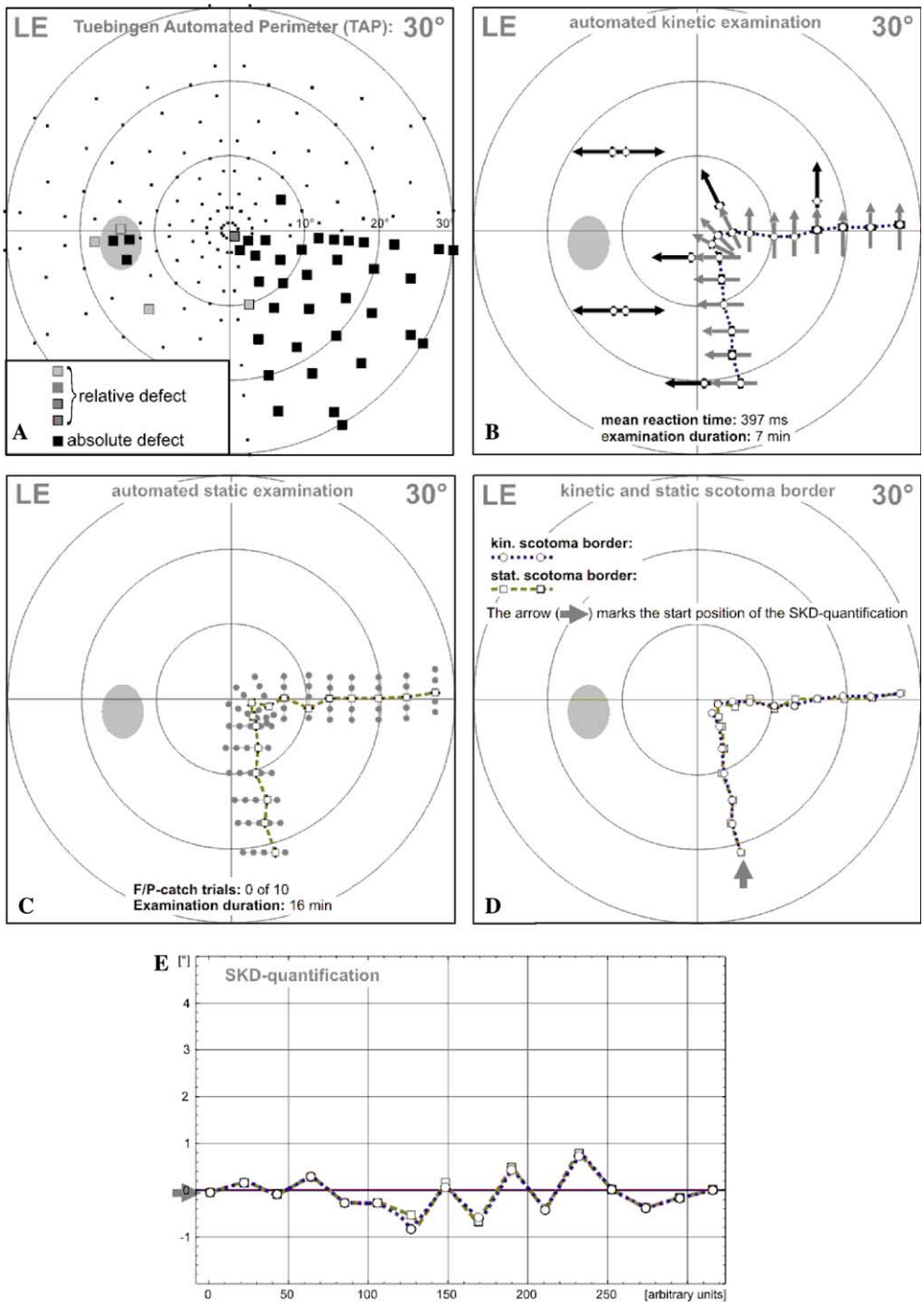

Fig. 6. Homonymous quadrantanopic visual field defect of a patient with a hemorrhage caused by a left partial occipital av-angioma. (A) Standard visual field: threshold oriented, slightly supraliminal perimetry (Tuebingen automated perimeter, TAP); (B) automated kinetic examination; (C) automated static examination; (D) comparison of kinetic and static examination result; (E) graph of SKD quantification.

examination found a maximum SKD of 2.8° with no negative SKD values.

The third patient to be illustrated (female; 34 years) suffered from an intracranial hemorrhage arising from a left partial occipital arteriovenous malformation. Her vascular malformation was treated by transluminal catheterization and embolisation. Initially, she showed a complete homonymous hemianopia to the right, which then regressed to a homonymous quadrantanopia (lower right quadrant) within a few days. There was no further regression in the size of the scotoma over the following 17 months prior to the SKD examination. Figs. 6A–E show the results of the examination: a very steep border from seeing to non-seeing parts in her visual field. There is no appreciable difference in the course of the static and kinetic scotoma border, thus SKD is very small (maximum 0.7°, minimum −0.8°).

3.2. Stato-kinetic dissociation

In summary all patients showed varying levels of SKD along the margins of their scotomas. The maximum local positive SKD value in the pooled data from all patients was 13.5°. Eight out of fifteen patients showed a locally negative SKD (maximum −1.2°). Both methods revealed considerable inter- and intraindividual variations of SKD along the borders of scotomas associated with differing mechanisms of visual field loss.

3.3. Individual reaction times, catch trials, duration of examinations, and retest reliability

Evaluation of the individual reaction times for each patient found considerable *intra*individual variance. Minimum mean RT was 384 ms and maximum 715 ms, showing again the wide range of *inter*individual mean reaction times.

The occurrence of false-positive answers was remarkably low: In only 1 out of 20 examinations there were 2 (out of 25) catch trials documented as being falsely positive (8%), in all other examinations this value was 0. These results in combination with the reasonably small dispersion of static thresholds indicate a high level of reliability in the responses of all patients.

Duration of the manual kinetic and static examinations varied between 8 and 10 min. The automated kinetic examination took 5–8 min, while the automated static examination lasted 15–18 min. The total time for the examination with manual testing, assignment of two individually adjusted sets of vectors, automated kinetic and static perimetry along the 16 vectors, and some short resting breaks between tests took about 1 h. Because of the interindividual differences between patients in responding to the kinetic and static stimuli and the need for rest breaks, it is not possible to give a more definite estimate of the time needed for the completion of testing for a single subject.

For estimation of retest reliability one patient in each of the three groups was examined at two separated times, one patient with retinitis pigmentosa was tested three times. The kinetic and static results of these three examinations of the patient with retinitis pigmentosa are shown in Figs. 7A and B. The differences between the first two examination results of the re-tested patients were −0.07 pointwise (SD 2.52) and −0.13 (SD 0.33) casewise for SKD based on the kinetic scotoma border. Averaging over all points of a patient enhanced correlation from 0.31 to 0.78.

4. Discussion

4.1. Evaluation of SKD

When Riddoch first described the phenomenon of stato-kinetic dissociation, a "quantification" was done by drawing the results of the static and kinetic examinations on the same sheet of paper (Riddoch, 1917). Using this simple method, SKD was estimated with the help of a degree scale. A more exact measurement and comparison of local SKD with this method was not possible: On the one hand, the McHardy Perimeter (which Riddoch used) and the Goldmann Perimeter, (which is used most often for kinetic perimetry) are characterized by a relatively low spatial resolution, especially in the central portions of the visual field. This has limited a more accurate determination of SKD, which might be the principal reason for the relatively sparse numbers of reported cases in the literature. Furthermore, when using manual kinetic perimetry, several examiner-dependent effects must be considered: The individual reaction times of the patient and the examiner are compounded. This may result in a systematic error in localizing the border of a scotoma, falsely moving it into seeing portions of the visual field. With higher stimulus velocities this effect would be amplified (Fankhauser, 1969; Schiefer et al., 1999, 2001c; Schiller et al., 1999). Additionally, with manual con-

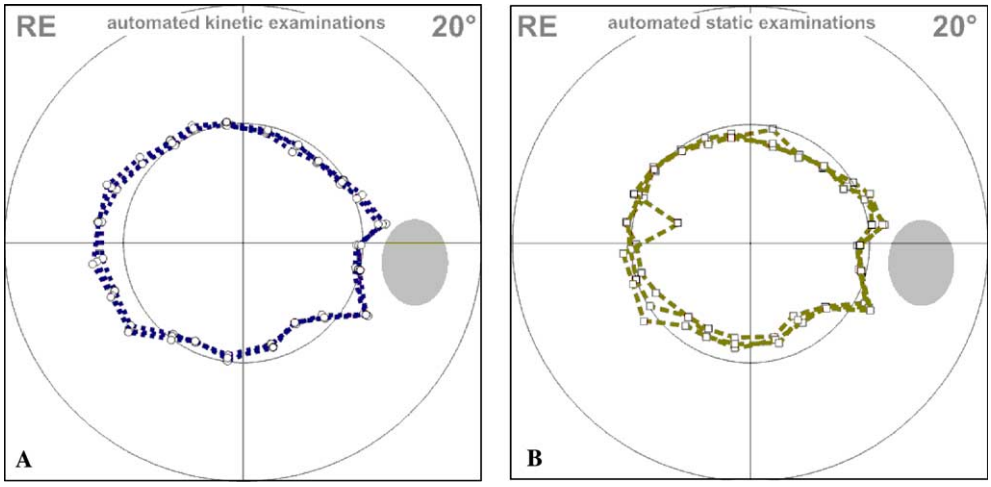

Fig. 7. (A) Results of the three kinetic examinations of a patient with retinitis pigmentosa; (B) results of the three static examinations of a patient with retinitis pigmentosa. In the kinetic as well as in the static examinations there are remarkably small differences in the localisations of the particular thresholds. Two of these examinations were carried out within a few hours, the third one week after the others.

trol of stimulus presentation, the angular velocity of a stimulus is not likely to be constant, and the results of the examination will depend heavily on the examiner's skill and experience.

Recent development of new (automated) perimeters has led to a segregation of static and kinetic examination procedures. As a result, two different devices must be used in order to get optimum results. Until now, this has been a major hindrance to the accurate quantification of SKD, and has limited the comparability of kinetic and static measures along the borders of visual field defects. With the method presented here, this limitation can be overcome. When using the TCC, the examiner has the option of choosing optimal vector locations and orientations. Each kinetic stimulus will be moved with a *constant* angular velocity (Schiefer et al., 2001a, 2001b), and the principles laid down by Hans Goldmann for accurate kinetic perimetry are complied with, namely that every scotoma border should be crossed as perpendicularly as possible with a constant angular velocity of stimulus movement (Goldmann, 1945a, 1945b). In addition, we are now able to correct for variations in individual reaction times.

4.2. Extent of SKD

The results presented here are characterized by a comparatively small SKD. One reason for this might have been the patients' selection criteria: stable visual field defects were a selection criterion for participation in this study. Another reason might be the comparatively low angular velocity of the kinetic stimuli of 2°/s. There are suggestions in the literature that increasing angular velocities of kinetic stimulus movement may amplify SKD (ffytche et al., 1995; Weiskrantz, 1995)—even when thresholds are corrected for reaction times. Furthermore, there have been no methods to correct for examiner and patient reaction times. The reaction time of the patient and the reaction time of the examiner both tend to shift threshold locations during conventional kinetic examinations. Kinetic threshold locations are shifted in the direction of motion of the moving stimulus. Depending on its extent, this effect can bias the results of an entire examination. The potential for this effect should always be considered. The method presented here offers a standardized form for SKD quantification with several restrictions. Because of the small case numbers, and in some cases inhomogeneous groups of patients, we did not perform any further comparative statistical evaluations. Future studies with larger groups of subjects and higher kinetic stimulus velocities are needed in order to estimate the range of SKD in various groups of patients and healthy subjects.

4.3. Clinical practicality

This study was designed with the intent of developing a method for the quantification of an important pathophysiologic change in the visual field. All subjects in this study were able to complete both static and kinetic testing within a reasonably short period of time, and did so without any apparent confusion. However, all patients in this study were relatively experienced perimetric subjects, and the use of naive subjects will be needed to confirm the practicality of the method.

The total examination times of about 1 h (including short rest breaks) are acceptable only when studying small numbers of patients with clinical disorders that suggest the presence of SKD. The 1 h duration accounts for the use of only one kinetic stimulus intensity and only for the study of a limited region of interest. Examination time is extended for approximately 30 min for each additional stimulus variable (size, luminance, or angular velocity). We do not know yet whether the use of multiple stimulus variables would add clinically relevant information. Furthermore, it is unknown whether restriction of the examination to a region of interest is sufficient for evaluating the SKD produced by diseases of the afferent visual pathways. Future studies will be designed to provide further information about the incidence and prevalence of SKD.

4.4. Outlook

The method described here allows for specification and control of several important perimetric variables: region of interest in the visual field; stimulus velocities for kinetic testing; corrections for variable reaction times; orientation, position and length of SKD vectors; and control of patients' visual fixation. This combination of controlled variables should greatly improve on the capabilities of conventional kinetic and automated static perimetry. However, the use of a campimetric device limits the examination area to the central visual field region of less than 34° of eccentricity. As a consequence, the peripheral visual field cannot be examined. In order to establish this new method in everyday clinical routine without any "restriction of eccentricity", the technique described here for automated assessment of SKD will be adapted for use with the Octopus 101 perimeter (HAAG-STREIT, Koeniz, Switzerland). At the moment this perimeter is the only commercially available automated 'full-field' cupola instrument that allows the examiner to specify the velocity and direction of kinetic stimuli under consideration of individual reaction time. It should allow for the direct transfer and exact duplication of the TCC method used in this study. Use of the Octopus instrument would also allow the introduction of a wider range of light adaptation and stimulus intensities.

4.5. Conclusion

By using a single perimetric device when examining with static and kinetic perimetric stimuli, local SKD can be measured and quantified with an improved level of precision. With this in mind, we developed the above described algorithm for automated quantification of local SKD. In addition to allowing more precise determinations of SKD, the

algorithm also incorporates features that limit the extent of artificially high values for SKD that can be associated with the sometimes complex geometry of visual field defects.

The main limitation of the method is the long examination time, which might be a problem for patients with acute diseases, such as those with cerebrovascular infarctions, in which the existence or absence of SKD might be an important prognostic factor.

Our primary intent was to develop a tool to measure SKD in a standardized and easily useful way. With use of a standardized automated method, such as the one introduced in this work, comparison of separate examinations is feasible and should make the data obtained with different perimetric devices more easily comparable. Although the initial data reported here are promising, it was not the intent of the authors to address the causes or significance of widely varying SKD values. Rather, our intent was to describe a new diagnostic tool, which may help to provide insight into the mechanisms underlying SKD. These are the topics to be addressed in further studies.

Acknowledgments

The authors thank T.J. Dietrich and B. Selig for their support in completing this study.

References

Aulhorn, E., & Karmeyer, H. (1977). Frequency distribution in early glaucomatous visual field defects. *Documenta Ophthalmologica*, 75–83.

Barbur, J. L., Watson, J. D. G., Frackowiak, R. S. J., & Zeki, S. (1993). Conscious vision without V1. *Brain, 116*, 1293–1302.

Benevento, L. A., & Yoshida, K. (1981). The afferent and efferent organization of the lateral geniculo-prestriate pathways in the macaque monkey. *Journal of Comparative Neurology, 203*, 455–474.

Bullier, J., & Kennedy, H. (1983). Projection of the lateral geniculate nucleus onto cortical area V2 in the macaque monkey. *Experimental Brain Research, 53*, 168–172.

Charlier, J. R., Defoort, S., Rouland, J. F., & Hache, J. C. (1989). Comparison of automated kinetic and static visual fields in neuro-ophthalmology patients. In A. Heijl (Ed.), *Perimetry update 1988/1989* (pp. 3–8). Amsterdam/Berkeley/Milano: Kugler & Ghedini.

Cowey, A., & Stoerig, P. (1991). The neurobiology of blindsight. *Trends in Neurosciences, 14*, 140–145.

Dietrich, T. J., Selig, B., Friedrich, M., Benda, N., & Schiefer, U. (1996). Calibration routines for video display units for perimetric examinations. *German Journal of Ophthalmology, 5*(Suppl. 1), 125.

Fankhauser, F. (1969). Kinetische Perimetrie. *Ophthalmologica, 158*, 406–418.

ffytche, D. H., Guy, C. N., & Zeki, S. (1995). The parallel visual motion inputs into areas V1 and V5 of human cerebral cortex. *Brain, 118*, 1375–1394.

ffytche, D. H., Guy, C. N., & Zeki, S. (1996). Motion response from a blind hemifield. *Brain, 119*, 1971–1982.

Finkelstein, J. I., & Johnson, L. N. (1989). Relative scotoma and statokinetic dissociation (Riddoch's phenomenon) from occipital lobe dysfunction. *Annual Meeting of the Pennsylvania Academy of Ophthalmology and Otolaryngology, 41*, 789–791.

Gandolfo, E. (1996). Stato-kinetic dissociation in subjects with normal and abnormal visual fields. *European Journal of Ophthalmology, 6*, 408–414.

Gandolfo, E., Rossi, F., Ermini, D., & Zingirian, M. (1995). Early perimetric diagnosis of glaucoma by stato-kinetic dissociation. In R. P. Mills & M. Wall (Eds.), *Perimetry update 1994/95* (Vol. 1994/95, pp. 271–276). Amsterdam/New York: Kugler.

Goldmann, H. (1945a). Ein selbstregistrierendes Projektionskugelperimeter. *Ophthalmologica, 109*, 71–79.

Goldmann, H. (1945b). Grundlagen exakter Perimetrie. *Ophthalmologica, 109*, 57–70.

Hudson, C., & Wild, J. M. (1992). Assessment of Physiologic Statokinetic Dissociation by Automated Perimetry. *Investigative Ophthalmology & Visual Science, 33*, 3162–3168.

Katsumori, N., Bun, J., Shirabe, H., & Mizokami, K. (1991). Statokinetic dissociation in glaucomatous peripheral visual damage. In R. P. Mills & A. Heijl (Eds.), *Perimetry update 1990/1991* (pp. 503–507). Amsterdam/New York: Kugler.

Krastel, H., Auffarth, G. U., Glaser, N., Beitzinger, M., & Alexandridis, E. (1996). Häufigkeit und Ausprägung des Riddoch-Phänomens (statokinetische Dissoziation) in der Perimetrie bei Netzhaut-, Sehnerv- und cerebralen Erkrankungen. *Der Ophthalmologe, 93*(Suppl. 1), 152.

Lee, B. B. (1993). Macaque ganglion cells and spatial vision. *Progress in Brain Research, 95*, 33–43.

Livingstone, M. S., & Hubel, D. H. (1984). Specificity of intrinsic connections in primate primary visual cortex. *Journal of Neuroscience, 4*, 2830–2835.

Livingstone, M. S., & Hubel, D. H. (1988). Segregation of form, color, movement, and depth: anatomy, physiology, and perception. *Science, 40*, 740–749.

Merigan, W. H., & Maunsell, J. H. R. (1990). Macaque vision after magnocellular lateral geniculate lesions. *Visual Neuroscience, 5*, 347–352.

Osako, M., Casson, E. J., Johnson, C. A., Huang, P., & Keltner, J. L. (1991). Statokinetic dissociation: analysis of spatial and temporal characteristics by perimetry. In R. P. Mills & A. Heijl (Eds.), *Perimetry update 1990/1991* (pp. 129–134). Amsterdam/New York: Kugler.

Riddoch, G. (1917). Dissociation of visual perceptions due to occipital injuries. *with especial reference to appreciation of movement. Brain, 40*, 15–57.

Safran, A. B., & Glaser, J. S. (1980). Statokinetic dissociation in lesions of the anterior visual pathways. *Archives of Ophthalmology, 98*, 291–295.

Schiefer, U., Schiller, J., Dietrich, T. J., Besch, D., Paetzold, J., & Vonthein, R. (2001a). Evaluation of advanced visual field loss with computer-assisted kinetic perimetry. In M. Wall & R. P. Mills (Eds.), *Perimetry update 2000/2001* (pp. 131–136). Hague: Kugler.

Schiefer, U., Schiller, J., Paetzold, J., Dietrich, T. J., Vonthein, R., & Besch, D. (2001b). Evaluation ausgedehnter Gesichtsfelddefekte mittels computerassistierter kinetischer Perimetrie. *Klinische Monatsblätter für Augenheilkunde, 218*, 13–20.

Schiefer, U., Schiller, J., Selig, B., Dietrich, T. J., Flad, M., Stumpp, F., et al. (1999). How does reaction time depend on eccentricity and luminance of kinetic targets?—A [video-] campimetric study in young normal volunteers. *Investigative Ophthalmology and Visual Science, 40*, 71 Abstract.

Schiefer, U., & Stercken-Sorrenti, G. (1993). Ein neues Rauschfeldkampimeter. *Klinische Monatsblätter für Augenheilkunde, 202*, 60–63.

Schiefer, U., Strasburger, H., Becker, S. T., Vonthein, R., Dietrich, T. J., Schiller, J., et al. (2001c). Reaction time in automated kinetic perimetry: Effects of stimulus luminance, eccentricity, and movement direction. *Vision Research, 41*(16), 2157–2164.

Schiller, J., Selig, B., Dietrich, T. J., Becker, S. T., Stumpp, F., Dietz, K., et al. (1999). Does direction of linear target motion influence reaction time?—A campimetric study using automated kinetic stimuli. *Investigative Ophthalmology and Visual Science, 40*, 845 (Abstract).

Tsutsui, J., Ichihashi, K., & Kimura, H. (1984). Dynamic topography of visual evoked potentials and extrageniculate projection in case of Riddoch phenomenon. *Japanese Journal of Ophthalmology, 28*, 20–30.

Wabbels, B., Schiefer, U., Treutwein, B., Benda, N., & Strecken-Sorrenti, G. (1995). Automated perimetry with bright and dark stimuli. *German Journal of Ophthalmology, 4*, 2217–2221.

Wedemeyer, L., Johnson, C. A., & Keltner, J. L. (1989). Statokinetic dissociation in optic nerve disease. In A. Heijl (Ed.), *Perimetry update 1988/*

1989 (Vol. 1989, p. 914). Amsterdam/Berkeley/Milano: Kugler & Ghedini.

Weiskrantz, L., Warrington, E. K., Sanders, M. D., & Marshall, J. (1974). Visual capacity in the hemianopic field following a restricted occipital ablation. *Brain, 97*, 709–728.

Weiskrantz, L. (1995). Blindsight—Not an island unto itself. *Current Directions in Psychological Science, 4*, 146–151.

Weiskrantz, L. (1996). Blindsight revisited. *Current Opinion in Neurobiology, 6*, 215–220.

Yabuki, K., Sakai, M., Suzumura, H., Endo, N., & Matsuo, H. (1989). A comparison of kinetic and static perimetry for lesions in the visual pathway. In A. Heijl (Ed.), *Perimetry update 1988/1989*. Amsterdam/Berkeley/Milano: Kugler & Ghedini.

Yukie, M., & Iwai, E. (1981). Direct projection from the dorsal lateral geniculate nucleus to the prestriate cortex in macaque monkeys. *The Journal of Comparative Neurology, 201*, 81–97.

Zappia, R. J., Enoch, J. M., Stamper, R., Winkelman, J. Z., & Gay, J. (1971). The Riddoch phenomenon revealed in non-occipital lobe lesions. *British Journal of Ophthalmology, 55*, 416–420.

Zeki, S. M. (1978). Functional specialisation in the visual cortex of the rhesus monkey. *Nature, 274*, 423–428.

Zeki, S., & ffytche, D. H. (1998). The Riddoch syndrome: Insights into the neurobiology of conscious vision. *Brain, 121*, 24–45.

Zihl, J. (1980). "Blindsight": Improvement of visually guided eye movements by systematic practice in patients with cerebral blindness. *Neuropsychologia, 18*, 71–77.